Available online at www.sciencedirect.com
SCIENCE DIRECT®
Carbohydrate Research 340 (2005) 889–905
Carbohydrate RESEARCH

Water T_2 relaxation in sugar solutions

Deborah Fabri, Martin A. K. Williams† and Thomas K. Halstead*

Department of Chemistry, University of York, Heslington, York YO19 6AL, UK

Received 17 October 2004; accepted 27 January 2005

Dedicated to Professor David A. Brant

Abstract—^{1}H spin–spin relaxation times of water were measured with the CPMG sequence in dilute aqueous solutions of glucitol, mannitol, glycerol, glycol, the methyl D-pyranosides of α-glucose, β-glucose, α-galactose, β-galactose, α-xylose, β-xylose, β-arabinose and sucrose, α,α-trehalose, β-maltose, maltotriose and maltoheptaose. The relaxation-time dispersion was measured by varying the CPMG pulse spacing, τ. These data were interpreted by means of the Carver–Richards model in which exchange between water protons and labile solute hydroxyl protons provides a significant contribution to the relaxation. From the dependences on temperature and τ, parameters characteristic of the pool of hydroxyls belonging to a given solute were extracted by nonlinear regression, including: the fraction of exchangeable protons, P, the chemical-shift difference between water protons and hydroxyl protons, $\delta\omega$, the intrinsic spin–spin relaxation time, T_2, and the chemical exchange rate, k. These solute-specific parameters are related, respectively, to the concentration, identity, mobility and exchange life-time of the hydroxyl site. At 298 K, values of $\delta\omega$, T_2 and k were found to be of the order of 1 ppm, 100 ms and 1000 s^{-1}, respectively. Effects of molecular size, conformation and solute concentration were investigated. The exchange mechanism was characterised by Eyring activation enthalpies and entropies with values in the ranges 50–70 kJ mol^{-1} and −10 to 60 J K^{-1} mol^{-1}, respectively.

Keywords: Polyols; Methyl glycosides of monosaccharides; Sucrose; Trehalose; Oligosaccharides; ^{1}H NMR CPMG relaxation dispersion; Proton exchange

1. Introduction

The interaction of carbohydrates with their surroundings in aqueous solutions and gels and crystalline hydrates, is strongly influenced by the properties of their hydroxyl groups. High-resolution NMR spectroscopy is widely used to investigate the structure and dynamics of carbohydrates in solution,[1] and, besides the conventional application of ^{1}H NMR using C–H protons as probes, methods have also been developed to extract structural information from hydroxyl proton resonances.[2–11] NMR relaxation measurements can provide complementary information by probing the molecular dynamics of both solute and solvent. ^{1}H and, especially, ^{2}H and ^{17}O spin-lattice relaxation studies[12] are well suited to determine correlation times of molecular motions, but the last two methods generally require samples with some degree of enrichment. No enrichment, however, is needed for ^{1}H NMR studies of water protons.

In general, the ^{1}H NMR spin–spin relaxation rate, $1/T_2$, of the water protons in dilute aqueous solutions containing carbohydrates (and proteins) is enhanced relative to that in pure water. Water self-diffusion and chemical exchange of protons between the solvent water molecules and labile protons on the solute (mainly but not exclusively belonging to hydroxyl or amine groups) are sufficiently rapid in these solutions, even close to neutral pH, to ensure that the decay of the ^{1}H NMR transverse magnetisation is a single exponential characterised by a unique spin–spin relaxation rate $1/T_2$.[13–18] As a consequence of this exchange, the all-pervading

* Corresponding author. E-mail addresses: deborahfabri@hotmail.com; m.williams@massey.ac.nz; tkh1@york.ac.uk
† Present address: Massey University, Institute of Fundamental Science, Private Bag 11-222, Palmerston North, New Zealand.

0008-6215/$ - see front matter © 2005 Elsevier Ltd. All rights reserved.
doi:10.1016/j.carres.2005.01.034

water protons retain a memory of the various environments visited on the NMR timescale (T_2) and their relaxation behaviour can serve indirectly to monitor the dynamics and other properties of the solute. In particular, if the observed relaxation rate, $1/T_2$, is measured by using the Carr–Purcell–Meiboom–Gill (CPMG) pulse sequence, useful information about the properties of the labile hydroxyl sites on the carbohydrate may be extracted by a detailed analysis of the NMR response.

In homogeneous aqueous solutions of small carbohydrates, in which the water protons are exchanging with protons belonging to sites located on the solute, $1/T_2$ of the water protons, measured with the CPMG sequence, is given by Eq. 1

$$1/T_2 = 1/T_{2a} + f_{CR}(P_b, \delta\omega_b, k_b, T_{2b}, \tau). \quad (1)$$

The bulk water site is labelled a and the exchangeable hydroxyl site b. f_{CR} is a closed analytical function with five parameters, derived by Carver and Richards[19] and corrected by Hills et al.[13] For the hydroxyl sites, P_b is the fraction of exchangeable hydroxyl protons, k_b is the exchange rate between hydroxyls and bulk water, $\delta\omega_b$ is the hydroxyl chemical shift relative to bulk water and T_{2b} is the local spin–spin relaxation time of the hydroxyl protons. A shorter value of T_{2b} generally indicates a slower motion of the OH group. The fifth parameter, τ, is the inter-pulse (90°–180°) spacing in the CPMG sequence, that is, a variable under the control of the experimenter. It should be noted that 'bound' water, namely, anisotropically orienting water with a short residence time, detectable with, for instance, ^{17}O NMR, is not important for our model.

The various OH groups of a carbohydrate are not, in general, equivalent. When there is any significant variation in the quantities that parameterise the CR expression, the observed T_2-dispersion curve will be a sum of the individual curves associated with the component hydroxyls. It has been shown,[20] however, and this paper will provide further evidence, that fitting the dispersion curve to a single CR function can still provide useful information and that the extracted k_b and $\delta\omega_b$ are sample average values of the various hydroxyls, whereas P_b is a good indication of the total number of exchangeable protons. The extracted value of T_{2b} is more difficult to interpret as it is more heavily weighted by components in the millisecond range.

By exploiting the abundant and ubiquitous water molecules as molecular-level probes, the CR model has considerable potential in the investigation of mobility and accessibility of labile protons in aqueous media at physiological pH. In this paper, the CR model is used to analyse the water relaxation data of solutions containing small carbohydrate molecules, as model systems chosen in order to assist the interpretation of the results of a subsequent study on polysaccharides (manuscript in preparation).

Acyclic polyols are natural compounds found in plants and fruits[21] and are widely used in the food and pharmaceutical industries for their sweetening and hygroscopic properties.[22] In this study some acyclic polyols were chosen in order to compare their relaxation behaviour with that of the related aldoses. The main interest was to assess any effect of the conformational restrictions imposed by the ring formation on sugar mobility and on the proton-exchange process. Two hexitols were studied, D-glucitol (**1**) and D-mannitol (**2**), which are shown in schemes in the conformation they adopt in crystals.[22] Besides the hexitols, two smaller polyols, glycol and glycerol, were also studied in order to test whether there is a detectable effect of the chain length on any of the CR parameters. The effect of varying concentration was studied in somewhat more detail on glucitol.

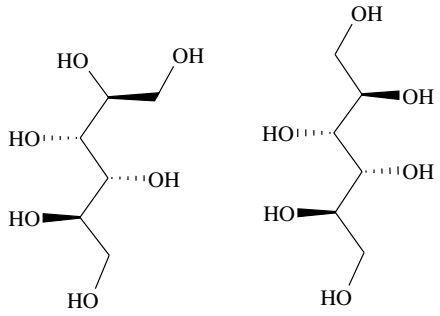

1 **2**

Studies on the hydration of polyhydroxy compounds[23–39] have revealed that slight differences in stereochemical configuration can significantly affect properties in solution. The stereospecificity of sugar hydration and related water-structuring effects are topics of interest also because of their application in biology, where functional processes are often based on the juxtaposition of hydrophobic and hydrophilic groups.

The methyl aldo-pentopyranosides and -hexopyranosides derived from α-glucose (**3**), β-glucose (**4**), α-galactose (**5**), β-galactose (**6**), α-xylose (**7**), β-xylose (**8**) and β-arabinose (**9**) were chosen as model compounds to study proton exchange between water and cyclic carbohydrates. The protection of the anomeric group avoids the complications arising from mutarotation, which would be difficult to take into account in a dynamics study in which the temperature is varied over a wide range. Also in the view of an anticipated comparison with maltodextrins, where glucose molecules are α-(1→4)-linked, the study of methyl glycosides, as opposed to parent monosaccharides, seemed more appropriate. The study of a variety of methyl glycosides is also aiming to explore the influence of stereochemistry on the exchange.

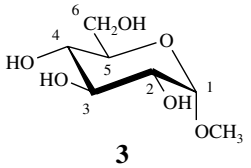

3

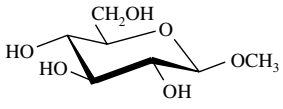

4

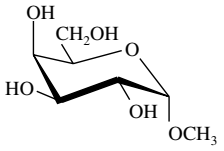

5

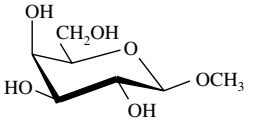

6

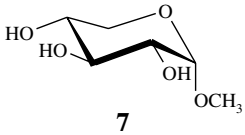

7

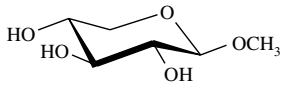

8

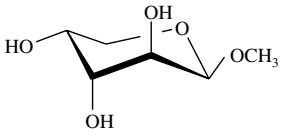

9

Two ever-interesting disaccharides are sucrose and α,α-trehalose, the former being relevant for its natural abundance and widespread applications, the latter for its intriguing capacity to act as bioprotector against dehydration and freezing. Although the solvation properties of these two sugars have been studied extensively for the past several decades, an understanding of the relation between molecular structure and solution properties is still not clear.[4,40–50] In the context of this relaxation study of proton-exchange processes, these two disaccharides appeared to be suitable candidates, since they are both nonreducing sugars with a glucosidic residue, linked to a fructose residue in sucrose (**10**) and glucose in α,α-trehalose (**11**).

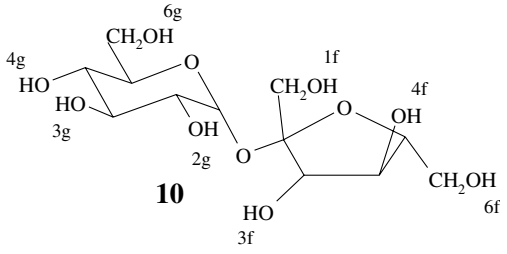

10

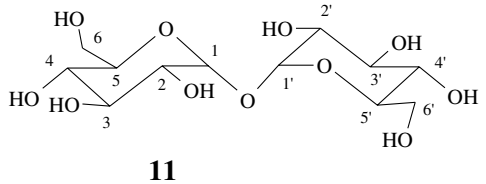

11

Since small sugars are the building blocks of polysaccharides, it is of interest to study some oligosaccharides of glucose that are α-(1→4) bonded, in order to examine the effect of chain length on the CR parameters. In view of the anticipated study on maltodextrins, the dimer, trimer and heptamer were chosen, namely: β-maltose (**12**), maltotriose (**13**) and maltoheptaose (**14**).

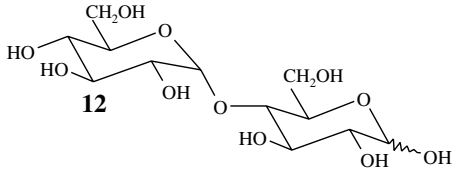

12

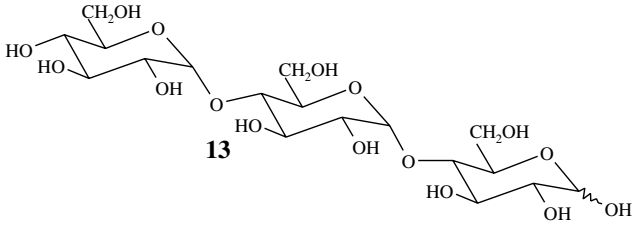

13

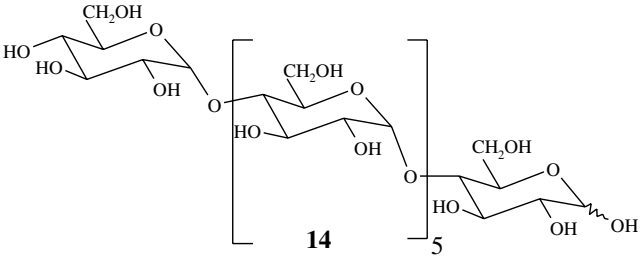

14

This paper forms part of a wider study of biopolymer mixtures, and a detailed description of the methodology developed to apply the CR model and an account of its further application to the investigation of polysaccharide (maltodextrin) solutions and gels will be presented elsewhere (manuscripts in preparation).

2. NMR T_2-dispersion analysis

2.1. Dispersion curves

The water T_2-dispersion curves for aqueous solutions of compounds **1**–**14** plus glycerol and glycol, were measured at various concentrations and temperatures, as described in Section 5.2.2.

A typical set of dispersion curves is shown for mannitol (**2**) as a 3D plot ($1/T_2(T,\tau)$) in Figure 1. The data were fitted to the CR expression and the parameters P_b, k_b^{298}, $\delta\omega_b^{298}$ and T_{2b}^{298}, as well as the parameters accounting for the temperature dependence, $\Delta^{\ddagger}H^{\ominus}$, $\Delta\delta\omega_b$ and E_b, were extracted as described in Section 5.3. The results are reported in Tables 1–4. It is often

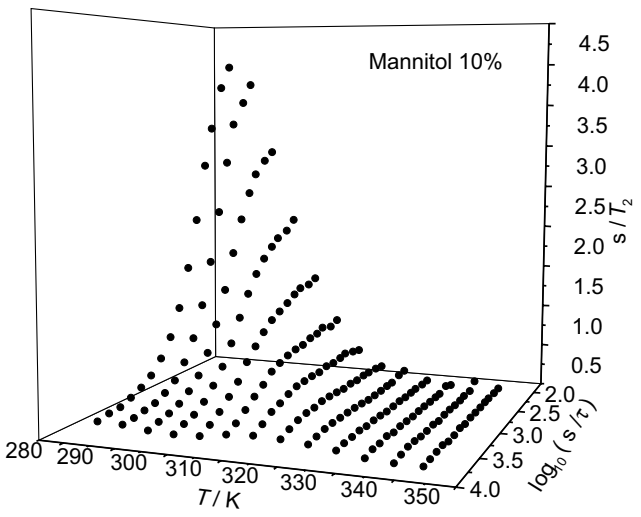

Figure 1. Spin–spin relaxation rate of a 10% w/w mannitol solution as a function of temperature and pulse spacing.

more convenient to plot the observed relaxation rates as a 2-D projection, thus, Figure 2 shows the same data for mannitol displayed as a function of pulse spacing, τ, and Figure 3 shows it plotted as a function of temperature. Some indication that the CR expression provides a good overall fit to the dispersion data is given by the correlation coefficients, R^2, given in Table 1, which are all >0.992, and visually by inspecting a typical fit, for example, for 10% mannitol shown in Figure 2, where the curves are best-fits for those data.

For maltose, maltotriose and maltoheptaose (**12**–**14**) at high temperatures an anomalous enhancement was observed, therefore only data below 328 K were fitted. The presence of another species that exchanged protons slowly except at high temperatures could account for this behaviour but none could be detected by either high-resolution NMR or MS. The phenomenon may be associated with the ability of these compounds to mutarotate, since they contain unprotected anomeric hydroxyls, and similar behaviour (data not presented) was observed for xylose, glucose, fructose and cellobiose. The fit for maltoheptaose, which has only one anomeric proton out of 23 exchangeable protons, is better than for either maltose or maltotriose, judging by the R^2 values (Table 1). This suggests that the anomeric OH proton present in these compounds has different characteristics compared with the other exchangeable protons.

There are two entries in each table for the most concentrated samples of glucitol, mannitol, sucrose and 5% maltose. These samples were used twice in consecutive experiments in order to check the reproducibility of measurements. Excellent agreement is found between parameters extracted from the data of the two runs, especially in the case of glucitol. Although the values of $\Delta^{\ddagger}H^{\ominus}$ are within experimental error (see Table 3), k_b^{298} increases by ~10% in the second run and $\Delta^{\ddagger}S^{\ominus}$ becomes more positive. This could be due to slow catalysis developing in older samples from contaminants slowly released by the glass of the NMR tube or, since the tubes are not sealed, absorbed from the air. The repeated measurements on the 20% maltose solutions, which were prepared separately, show slightly larger differences in the extracted parameters, which can be ascribed to some irreproducibility in sample preparation (mainly pH control) rather than to fitting errors.

2.2. Chemical shifts

The chemical-shift differences, $\delta\omega_b$, derived from the fits that are given in Table 1 are, for each carbohydrate, an average chemical-shift difference for all nonequivalent hydroxyl protons of the molecule. The values obtained were consistent within each class of compounds and a small but significant decrease of $\delta\omega_b^{298}$ with increasing concentration was observed in all samples that were studied at different concentrations, except Me β-galactopyranoside and Me α-xylopyranoside.

The temperature coefficients of the chemical-shift difference, $\Delta\delta\omega_b$, obtained from the fittings as per Eq. 7, are also given in Table 1. The values were in the range −1 to −8 ppb indicating that $\delta\omega_b^{298}$ was decreasing upon heating and that the change was less than −0.5 ppm over the 60 K range under investigation in this study.

2.3. Fraction of exchangeable protons

The fractions of exchangeable protons, P_b(experimental), determined by fitting and P_b(calculated), calculated from the concentration of the solutes, are reported in Table 2. The experimental values were always smaller than calculated ones.

2.4. Exchange rate

The parameters k_b^{298}, $\Delta^{\ddagger}H^{\ominus}$ and $\Delta^{\ddagger}S^{\ominus}$ that characterise the exchange process are shown in Table 3 and the values are discussed in more detail in Section 3.3.

On comparing samples of glucitol and mannitol ~10% w/w, some qualitative assessments of the CR parameters can be made even before fitting the data, by visual inspection of the observed relaxation rate. Figures 3 and 4 clearly show the progressive shift of the position of the $1/T_2$ maximum when τ is decreased. The height of the maximum, $P_b\delta\omega_b/2$, at the longest τ is similar in both figures, ~4 s^{-1}, implying that the samples have approximately the same concentration, P_b, and chemical-shift differences, $\delta\omega_b^{298}$. The temperature of this maximum, however, is different for the two samples indicating different exchange rates, k_b, and the fact that the maxima occur at lower temperatures for mannitol

Table 1. Chemical-shift differences and their temperature coefficients

Carbohydrate	% w/w	$\delta\omega_b^{298}$ (ppm)	$\Delta\delta\omega_b/K^{-1}$ (ppb)	R^{2a}
Glucitol	5.0	0.706 ± 0.022	−2.8 ± 1.1	0.9966
	10.1	0.677 ± 0.012	−1.8 ± 0.8	0.9982
	19.9	0.664 ± 0.012	−1.8 ± 0.7	0.9979
	19.9	0.664 ± 0.010	−1.6 ± 0.6	0.9985
Mannitol	10.0	0.720 ± 0.019	−2.7 ± 1.5	0.9976
	20.0	0.656 ± 0.012	−2.9 ± 0.9	0.9982
	20.0	0.649 ± 0.009	−1.2 ± 0.6	0.9992
Glycerol	16.6	0.698 ± 0.025	−1.1 ± 0.8	0.9963
Glycol	20.0	0.694 ± 0.018	−1.7 ± 1.0	0.9974
	21.5	0.793 ± 0.024	−2.8 ± 1.2	0.9978
Me α-glucopyranoside	10.0	1.121 ± 0.016	−2.5 ± 1.2	0.9991
	20.0	1.065 ± 0.018	−3.0 ± 1.3	0.9986
Me β-glucopyranoside	9.6	1.133 ± 0.015	−2.31 ± 1.0	0.9994
Me α-galactopyranoside	10.0	0.892 ± 0.012	−4.0 ± 0.8	0.9986
	19.9	0.842 ± 0.013	−3.8 ± 1.5	0.9969
Me β-galactopyranoside	10.0	0.986 ± 0.035	−3.4 ± 2.6	0.9924
	19.8	1.039 ± 0.035	−1.5 ± 1.4	0.9980
Me α-xylopyranoside	10.0	1.177 ± 0.021	−2.2 ± 0.8	0.9974
	20.0	1.269 ± 0.046	−7.9 ± 3.2	0.9960
Me β-xylopyranoside	19.7	1.177 ± 0.024	−7.9 ± 2.2	0.9953
Me β-arabinopyranoside	19.8	0.823 ± 0.020	−2.5 ± 1.2	0.9979
Sucrose	10.0	1.280 ± 0.028	−5.9 ± 1.6	0.9972
	20.0	1.142 ± 0.017	−2.5 ± 1.2	0.9987
	20.0	1.151 ± 0.014	−1.9 ± 0.9	0.9992
α,α-Trehalose	10.0	1.252 ± 0.036	−7.0 ± 2.0	0.9954
	19.9	1.209 ± 0.018	−1.7 ± 1.2	0.9986
β-Maltose	5.0	1.390 ± 0.041	−4.0[b]	0.9950
	5.0	1.370 ± 0.044	−4.0[b]	0.9948
	10.0	1.359 ± 0.029	−4.0[b]	0.9978
	20.0	1.306 ± 0.046	−4.4 ± 4.0	0.9974
	20.0	1.336 ± 0.050	−5.2 ± 2.2	0.9956
Maltotriose	9.9	1.371 ± 0.038	−8.0[b]	0.9977
	10.0	1.325 ± 0.038	−8.0[b]	0.9978
Maltoheptaose	19.8	1.307 ± 0.0178	−4.0[b]	0.9990

[a] Correlation coefficient.
[b] Parameter fixed during fitting.

shows that the corresponding exchange rates are higher for that sample.

2.5. Relaxation time

Values of the intrinsic spin–spin relaxation time at 298 K, T_{2b}^{298}, are given in Table 4 for all samples. Despite large uncertainty associated with some of the values for all samples, it is possible to see a trend going from polyols to methyl monosaccharide glycosides and to oligosaccharides, in which T_{2b}^{298} becomes shorter. Similarly, the decrease of T_{2b}^{298} with concentration observed for glucitol, mannitol and maltose is larger than the experimental uncertainties.

In a few cases the dispersion data were insensitive to the value of T_{2b}^{298} and this parameter (and sometimes also E_b) was fixed during the fitting procedure in order to extract values for the other parameters. This was necessary whenever the low temperature maximum of the relaxation rate at short pulse spacing occurred at a temperature at or below the limit of the accessible temperature window. Since this maximum occurs close to the temperature when $k_b = 1/T_{2b}$ this is more likely to happen when the exchange rate is high.

3. Discussion

3.1. Chemical shifts

The chemical-shift differences derived from the fitting with the CR expression, given in Table 1, were in good

Table 2. Fitted and calculated fraction of exchangeable protons (P_b) and their ratios

Carbohydrate	% w/w	10^3 P_b(experimental)	10^3 P_b(calculated)	$\frac{\text{Experimental}}{\text{Calculated}}$ (%)
Glucitol	5.0	12.5 ± 0.7	15.4	81.2
	10.1	27.8 ± 0.8	32.2	86.3
	19.9	54.8 ± 1.6	68.6	79.9
	19.9	54.6 ± 1.4	68.6	79.6
Mannitol	10.0	24.5 ± 1.1	31.9	76.8
	20.0	54.6 ± 1.8	69.0	79.1
	20.0	61.1 ± 1.6	69.0	88.6
Glycerol	16.6	47.0 ± 2.1	55.1	85.3
Glycol	20.0	43.0 ± 2.2	67.6	63.6
	21.5	33.5 ± 2.0	73.6	45.5
Me α-glucopyranoside	10.0	18.9 ± 0.4	20.2	93.6
	20.0	37.5 ± 0.9	44.3	84.7
Me β-glucopyranoside	9.6	19.2 ± 0.4	19.3	99.5
Me α-galactopyranoside	10.0	17.2 ± 0.3	20.2	85.1
	19.9	34.9 ± 1.2	44.0	79.3
Me β-galactopyranoside	10.0	19.3 ± 0.9	20.2	95.5
	19.8	34.3 ± 1.2	43.8	78.3
Me α-xylopyranoside	10.0	17.1 ± 0.4	17.9	95.5
	20.0	23.8 ± 2.3	39.5	60.3
Me β-xylopyranoside	19.7	35.0[a]	38.8	90.2
Me β-arabinopyranoside	19.8	35.4 ± 1.5	39.0	90.8
Sucrose	10.0	18.0 ± 0.6	22.8	78.9
	20.0	42.7 ± 0.9	50.0	85.4
	20.0	43.4 ± 0.8	50.0	86.8
α,α-Trehalose	10.0	19.3 ± 0.9	22.6	85.4
	19.9	42.2 ± 1.5	49.7	84.9
β-Maltose	5.0	9.8 ± 0.4	10.9	89.9
	5.0	11.9 ± 0.5	10.9	109.2
	10.0	21.3 ± 0.7	22.8	93.4
	20.0	43.8 ± 3.1	49.8	88.0
	20.0	42.2 ± 2.6	49.8	84.7
Maltotriose	9.9	17.3 ± 0.5	21.1	82.0
	10.0	16.3 ± 0.6	21.3	76.5
Maltoheptaose	19.8	31.8 ± 1.2	42.4	75.0

[a] Parameter fixed during the fitting.

agreement with the averages of shifts measured from high-resolution NMR spectra at sub- to ambient temperature. This result supports the interpretation that extracted values of $\delta\omega_b$ are approximately equal to the average shift of the constituent components weighted by their relative amounts.[20]

The $\delta\omega_b$ values of the polyols were consistent with those reported by various authors for the exocyclic hydroxyl protons of sugars in aqueous[2,51,52] and water/acetone-d_6[6] solutions.

Although in the two-site CR model no distinction is made between the chemical-shift differences of each OH, our data for the methyl glycosides (**3**–**11**) are in line with the high-resolution NMR measurements of Adams and Lerner.[6] As shown in Table 5, our values differ from those in Ref. 6 by up to 0.3 ppm, but this could be accounted for by the fact that in Ref. 6 the spectra were recorded at lower pH (5.5) and in a mixed solvent (1:2 v/v water–acetone-d_6).

The values of $\delta\omega_b^{298}$ for sucrose (**10**) are in good agreement with the average values for the hydroxyls: 1.13 (0.82 M in water at 267 K),[2] 1.08 (1.2 M in water at 264 K)[53] and 1.14 (25 mM in 1:2 (v/v) water–acetone-d_6 at 290 K),[6] when the differences in concentration, solvent and temperature are taken into account.

To the best of our knowledge, there are no data in the literature on the chemical shift of hydroxyl protons in the aqueous solutions of trehalose (**11**). The values given in Table 1 are, as expected, similar to the corresponding ones for Me α-glycopyranoside. Differences in hydration and hydrogen-bond strength, which induce a greater deshielding of the hydroxyl protons, could

Table 3. Experimental exchange rates, Eyring enthalpies and entropies of activation

Carbohydrate	% w/w	$k_b^{298}/10^3\ s^{-1}$	$\Delta^{\ddagger}H^{\ominus}$/kJ mol^{-1}	$\Delta^{\ddagger}S^{\ominus}$/J K^{-1} mol^{-1}	$k_b(T)$[a]/s^{-1}	$k(T)$[b]/s^{-1}
Glucitol	5.0	0.909 ± 0.032	64.4 ± 1.5	27.5 ± 5.0		
	10.1	0.655 ± 0.017	69.7 ± 1.1	42.4 ± 3.6		
	19.9	0.496 ± 0.012	57.0 ± 1.0	−2.3 ± 3.2		
	19.9	0.534 ± 0.012	57.9 ± 0.9	1.1 ± 2.9		
Mannitol	10.0	1.404 ± 0.061	71.7 ± 2.1	55.6 ± 6.9		
	20.0	0.857 ± 0.024	62.4 ± 1.2	20.4 ± 4.2		
	20.0	0.955 ± 0.019	62.9 ± 0.9	29.5 ± 2.9		
Glycerol	16.6	1.120 ± 0.039	53.3 ± 1.6	−7.9 ± 5.5		
Glycol	20.0	1.001 ± 0.033	56.9 ± 1.4	3.0 ± 4.8		
	21.5	1.680 ± 0.061	60.4 ± 1.7	19.2 ± 5.7		
Me α-glucopyranoside	10.0	1.738 ± 0.045	68.7 ± 1.1	47.4 ± 3.7	4.8 ± 1.3[c]	12[d]
	20.0	1.279 ± 0.033	66.5 ± 1.1	37.3 ± 3.8		
Me β-glucopyranoside	9.6	2.152 ± 0.043	69.1 ± 0.9	50.3 ± 3.1	59.4 ± 1.2[c]	18[d]
Me α-galactopyranoside	10.0	0.574 ± 0.012	67.8 ± 0.8	35.2 ± 2.8	16.9 ± 0.3[c]	12[d]
	19.9	0.873 ± 0.032	70.7 ± 1.6	48.2 ± 5.3	22.3 ± 0.8[c]	
Me β-galactopyranoside	10.0	0.675 ± 0.035	71.5 ± 2.2	48.9 ± 7.4		
	19.8	1.891 ± 0.077	64.1 ± 1.9	32.6 ± 6.3		
Me α-xylopyranoside	10.0	0.533 ± 0.012	62.3 ± 0.9	15.9 ± 3.1		
	20.0	2.211 ± 0.126	65.2 ± 2.6	37.7 ± 8.7		
Me β-xylopyranoside	19.7	1.569 ± 0.083	60.6 ± 2.2	19.4 ± 7.3		
Me β-arabinopyranoside	19.8	1.525 ± 0.053	66.5 ± 1.6	39.0 ± 5.4		
Sucrose	10.0	2.052 ± 0.067	64.5 ± 1.9	34.5 ± 6.2	173 ± 5.7[e]	12[f]
	20.0	1.076 ± 0.024	59.6 ± 0.9	12.8 ± 3.0	109 ± 2.4[e]	
	20.0	1.240 ± 0.022	60.1 ± 0.7	15.5 ± 2.5	123 ± 2.2[e]	
α,α-Trehalose	10.0	2.142 ± 0.095	64.5 ± 2.5	34.8 ± 8.4		
	19.9	3.006 ± 0.083	67.3 ± 1.6	47.3 ± 5.4		
β-Maltose	5.0	0.756 ± 0.022	74.2 ± 1.4	58.7 ± 4.6		
	5.0	1.183 ± 0.032	70.8 ± 1.5	51.1 ± 5.0		
	10.0	1.807 ± 0.051	64.0 ± 1.6	31.9 ± 5.3		
	20.0	2.635 ± 0.152	57.9 ± 2.4	14.5 ± 8.2		
	20.0	2.197 ± 0.112	52.1 ± 2.5	−6.6 ± 8.3		
Maltotriose	9.9	2.590 ± 0.071	70.7 ± 1.6	57.4 ± 5.5		
	10.0	2.325 ± 0.059	64.2 ± 1.5	34.7 ± 5.0		
Maltoheptaose	19.8	2.998 ± 0.055	55.3 ± 1.1	6.9 ± 3.7		

[a] This study, calculated with Eq. 6 from the corresponding k_b^{298}.
[b] Literature value.
[c] This study, rate calculated for 265 K.
[d] Averaged values for 265 K taken from Ref. 7. Sample concentration ca. 50 mM in 85% H_2O–15% $(CD_3)_2CO$.
[e] This study, rate calculated for 273 K.
[f] Averaged values for 273 K taken from Ref. 40. Sucrose 50 mM in 1:3 v/v acetone-d_6/water.

account for the slightly higher shifts observed for trehalose.

The $\delta\omega_b^{298}$ values for the oligosaccharide samples (**12**–**14**), given in Table 1 are higher than, for example, for compound **3**. This is due to the fact that the α and β anomeric OH protons resonate, respectively, about 2 and 2.8 ppm downfield from water[2,52,53] and therefore the weighted average chemical-shift differences over all hydroxyl protons is increased noticeably by this contribution. Note that both anomers are present in their equilibrium proportions. The values given in Table 1 are in good agreement with those of Ref. 53, measured from high-resolution spectra at 264 K. For maltoheptaose (**14**) where the contribution from the anomeric proton has little weight (1 in 23 exchangeables, compared with 1 in 8 for β-maltose), a lower $\delta\omega_b^{298}$ value indeed resulted from the fitting.

The effect of conformation on the chemical-shift differences is evident from the data on the methylated sugars. The α anomers of **3** and **5** have smaller chemical-shift differences compared with corresponding β anomers (**4** and **6**). This is caused by an upfield shift

Table 4. Intrinsic spin–spin relaxation times at 298 K and activation energies

Carbohydrate	% w/w	T_{2b}^{298}/s	E_b/kJ mol^{-1}
Glucitol	5.0	0.30 ± 0.06	9.3 ± 6.3
	10.1	0.32 ± 0.05	28.7 ± 9.3
	19.9	0.21 ± 0.02	17.6 ± 5.3
	19.9	0.22 ± 0.02	17.6 ± 4.9
Mannitol	10.0	0.35 ± 0.13	52.8 ± 18.7
	20.0	0.19 ± 0.02	21.0 ± 4.2
	20.0	0.21 ± 0.02	24.4 ± 3.3
Glycerol	16.6	0.32 ± 0.06	20.0[a]
Glycol	20.0	0.36 ± 0.08	18.5 ± 10.2
	21.5	0.22 ± 0.04	12.7 ± 4.6
Me α-glucopyranoside	10.0	0.18 ± 0.03	32.3 ± 11.2
	20.0	0.12 ± 0.01	19.6 ± 4.2
Me β-glucopyranoside	9.6	0.15[a]	23.0 ± 3.7
Me α-galactose	10.0	0.17 ± 0.02	11.8 ± 3.9
	19.9	0.16 ± 0.02	27.3 ± 7.7
Me β-galactopyranoside	10.0	0.19 ± 0.03	34.7 ± 23.9
	19.8	0.15[a]	21.9 ± 4.3
Me α-xylopyranoside	10.0	0.13 ± 0.02	32.0[a]
	20.0	0.10[a]	21.2 ± 4.0
Me β-xylopyranoside	19.7	0.10[a]	15.4 ± 5.80
Me β-arabinopyranoside	19.8	0.12 ± 0.01	19.2 ± 3.4
Sucrose	10.0	0.3[a]	15.4 ± 5.80
	20.0	0.12 ± 0.01	15.1 ± 4.2
	20.0	0.12 ± 0.01	18.4 ± 3.9
α,α-Trehalose	10.0	0.5[a]	15.0[a]
	19.9	0.2[a]	15.0[a]
β-Maltose	5.0	0.15 ± 0.07	24.1 ± 13.1
	5.0	0.12 ± 0.05	27.0 ± 13.0
	10.0	0.1[a]	25.0[a]
	20.0	0.8 ± 0.02	27.0 ± 9.9
	20.0	0.07 ± 0.01	27.0[a]
Maltotriose	9.9	0.1[a]	27.0 ± 5.9
	10.0	0.1[a]	27.6 ± 5.7
Maltoheptaose	19.8	0.040 ± 0.002	14.2 ± 1.5

[a] Parameter fixed during the fitting.

(towards water resonance) of the resonance of the equatorial OH proton in position 2 (see formula **3**) owing to the presence of the axial oxygen of the α-methyl group.[6] Me α-xylopyranoside (**7**) has a bigger shift than Me α-glycopyranoside (**3**), since it lacks the exocyclic OH (for which $\delta\omega_b^{298}$ is ~0.75 ppm).

Galactose and arabinose methyl glycosides have smaller chemical-shift differences compared with the ones for glucoside and xyloside, respectively. This is expected[6,53] as the result of additive upfield shift-effects (that is towards the water line) since axial hydroxyl protons: (i) resonate at higher field than equatorial ones, (ii) induce an upfield shift of the resonances of neighbouring equatorial hydroxyl protons and (iii) induce an upfield shift of second-next-neighbour equatorial OH protons. Both methyl galactoside and methyl arabinoside have axial hydroxyl groups (see formulas **5**, **6** and **9**) that are not present in methyl glucosides (**3**, **4**) and methyl xylosides (**7**, **8**). Adams and Lerner[6] were able to interpret quantitatively the reduced chemical-shift differences of Me galactoside with respect to Me glucoside. The low $\delta\omega_b$ of Me β-arabinoside found here can be explained in the same way since Me β-arabinoside, has two axial oxygen-bearing groups (–O–3H and –O–2H in the $^4C_1$ conformation, see formula **9**) and is therefore expected to display a smaller $\delta\omega_b^{298}$.

The decrease of $\delta\omega_b^{298}$ with increasing concentration is consistent with the findings for glucose over a similar range of concentration,[2] and for water–alcohol mixtures.[54] The effect was explained as being due to a scavenging effect by alcohol hydroxyls that form double H bonds with nonhydrogen-bonded water, causing a

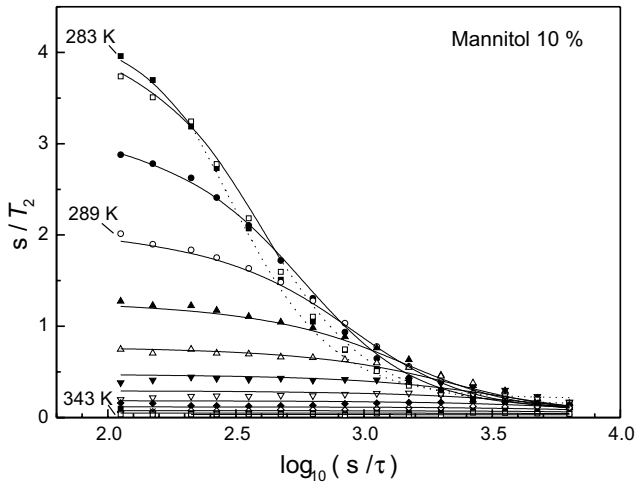

Figure 2. Relaxation rate of a 10% w/w mannitol solution, same data as in Figure 1, plotted as a function of pulse spacing. Experimental data (symbols) and corresponding CR fits calculated using parameters from Tables 1–4 (solid and dotted lines).

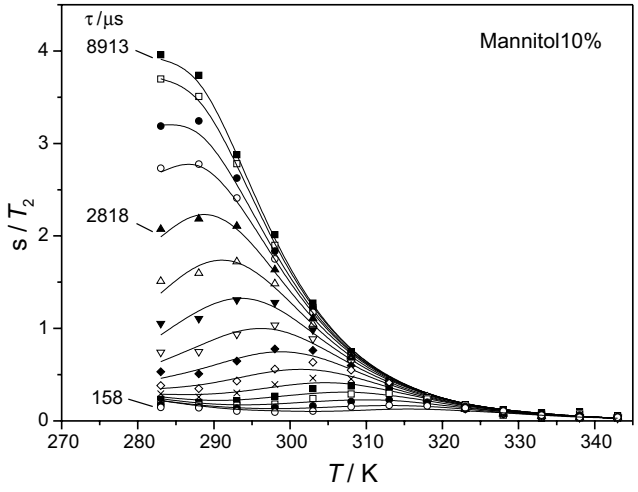

Figure 3. Relaxation rate of 10% w/w mannitol solution, same data as in Figure 1, plotted as a function of temperature. Experimental data (symbols) and corresponding CR fits calculated using parameters from Tables 1–4 (solid lines).

different extent of deshielding for water protons and alcohol hydroxyl protons in that concentration regime. It appears that a similar explanation, essentially based on the interplay of the acid–base properties of water and solute, would apply to our results.

The few published data on the temperature dependence of the chemical-shift difference, $\Delta\delta\omega_b$, are not in complete agreement,[6,51,52] However, Harvey and Symons[2] found that in glucose solutions, water has a slightly smaller upfield shift on heating than the hydroxyl protons, as a result the line separation decreases at higher temperatures, in agreement with our findings.

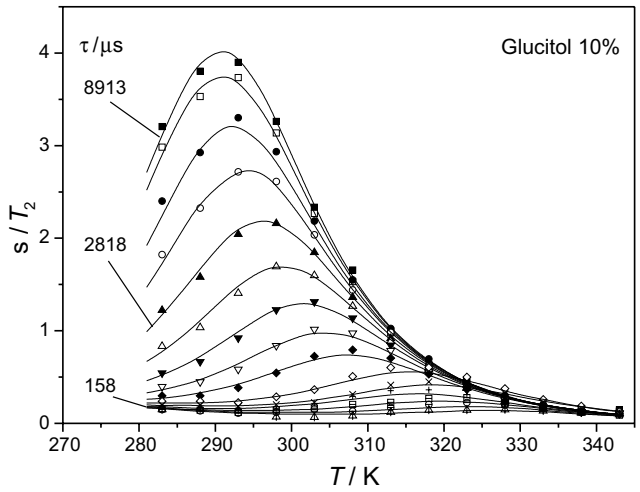

Figure 4. Relaxation rate of 10% w/w glucitol solution. Experimental data (symbols) and corresponding CR fits calculated using parameters from Tables 1–4 (solid lines).

Table 5. Chemical shift differences for methyl glucoside and methyl galactoside

	$\delta\omega^{250\,a}$	$\delta\omega_b^{250\,b}$
Me α-glucopyranoside	0.982[c]	1.24 ± 0.02
Me β-glucopyranoside	1.102	1.24 ± 0.02
Me α-galactopyranoside	0.767	1.08 ± 0.02
Me β-galactopyranoside	0.880	1.15 ± 0.04

[a] Averaged values from Ref. 6, measured at 250 K.
[b] Calculated for 250 K using values from Table 1.
[c] All values in ppm.

3.2. Fraction of exchangeable protons

The fractions of exchangeable protons, P_b, extracted from the fitting of the hexitol dispersion curves are up to 25% smaller than those calculated from the nominal concentration of the samples (see Table 2). In the case of the smaller polyols, the difference between fitted and calculated P_b values is about 15% for glycerol and greater than 45% for glycol. Considering that in glucitol (**1**) and mannitol (**2**) each OH contributes about 17% of P_b, while the contribution in glycerol is 33% and in glycol 50%, the results in Table 2 are consistent, for the hexitols and glycol, with one OH from each molecule not participating in the exchange, that is, it is exchanging at a lower rate ($k_b < 100\ s^{-1}$) than the others and therefore is not detectable by our measurements. The unavailability of protons for exchange, or their low rate of exchange, could be due to them being engaged in hydrogen bonds that persist on the time scale of the exchange (milliseconds). Intramolecular hydrogen-bond formation has indeed been reported for glycol in crystals and nonaqueous solvents in IR[55] and NMR studies,[5] but both NMR measurements[56] and theoretical calculations[57] have excluded

the existence of long-lived intramolecular H bonds in aqueous solutions, where stabilisation results instead from hydration effects. It seems therefore more likely that availability for exchange is dependent on conformational factors. This suggestion is supported also by the results of the methyl glycosides, for which the differences between the fitted and calculated values are less pronounced, and are bigger at the highest concentration. This observation supports the suggestion for a stereospecific model of exchange, although it is not possible to say which proton could be exchanging slowly. For a given sugar, the difference between experimental and calculated P_b is bigger (i) at the highest concentration and (ii) in the α-anomeric form.

For sucrose (**10**) fitted P_b values are about 80% of nominal value, suggesting that one out of eight hydroxyl protons does not exchange, or exchanges much more slowly, with water. The conformations of sucrose[44,45] and trehalose (**11**)[49] in solution are still a matter of debate, but it is now generally accepted that the intramolecular hydrogen bonds of the crystal structure are entirely substituted by interactions with the solvent. Moreover, the agreement between NMR and MD studies suggests[44,45] that in sucrose solutions water molecules can act as inter-residue bridge between the hydroxyl group in position 2 of the glucose residue (O-2g, see formula **10**) and that in position either 1 or 3 of the fructose residue (O-lf or O-3f, see formula **10**). The time-scale of the characteristic residence time of bridging water molecules, from MD calculations,[45] is of the order of picoseconds, thus much shorter than the exchange lifetime, $1/k_b$. It must be remembered that the exchange of water between the bulk and the bridging site is just the first step in the process of proton exchange. For proton exchange to occur, an O–H bond must break and a proton be transferred from the donor to the acceptor oxygen. There is a high activation barrier for this process (ca. 55–65 kJ mol^{-1}) thus it proceeds on a much longer timescale than the water exchange.

3.3. Exchange rate

Simulations[20] have shown that extracted values of k_b^{298} (and $\delta\omega_b$) are a useful indication of the average of those of the constituent components, weighted by their relative amounts.

Table 3 shows that the k_b^{298} values for glucitol (**1**) and mannitol (**2**) decrease with increasing concentration and are lower than for glycerol and glycol at comparable concentrations. The values of k_b^{298} for the methyl glycoside solutions, shown in Table 3, are in the range expected for carbohydrate solutions and gels.[16,58] The α anomers of Me glucoside and Me galactoside have lower exchange rates than the corresponding β anomers. However, any generalisation of particular trends should be done carefully in the case of k_b^{298} since the exchange of these samples appeared quite sensitive to adventitious catalysis. This was noticed by Harvey and Symons[2] in their work on monosaccharides and, indeed, in some high-resolution NMR studies[6–8,40] extreme precautions were taken in order to avoid catalysis and slow down the exchange enough to allow separate resonances for hydroxyl and water protons to be recorded. On the other hand, the advantage of the CR method applied to relaxation rates measured with the CPMG pulse sequence, is that measurement of the exchange rate can be made in the fast exchange limit ($k_b > \delta\omega_b$), in which the resonances of the various sugar OH protons and water collapse into a single averaged line. Therefore, the protocol adopted by some authors[40] for high-resolution studies, while essential for their purposes, was considered beyond the routine and the necessity of this study. Moreover, both the simulations[20] and the experimental results (not reported here) showed that, in all but a few cases, the other CR parameters can be fitted reliably, independent of the value of k_b^{298}. Consequently, the values obtained for the exchange rates will be regarded with some circumspection and in the discussion their absolute values will not be relied on when drawing the main conclusions.

For all compounds, the Eyring enthalpies of activation, $\Delta^{\ddagger}H^{\ominus}$, shown in Table 3, are approximately in the range 50–70 kJ mol^{-1}. Eyring entropies of activation, $\Delta^{\ddagger}S^{\ominus}$ are generally positive, indicating that the formation of the transition state involves an increase in disorder. $\Delta^{\ddagger}S^{\ominus}$ tends to decrease in magnitude as the concentration increases and, in the case of glucitol, glycerol and maltose may become negative. Exceptions are glycol, Me α-galactoside, Me α-xyloside and trehalose, where $\Delta^{\ddagger}S^{\ominus}$ becomes more positive as the concentration increases.

In order to compare our results with the small amount of literature data available on exchange of hydroxyl protons, an extrapolation to 265 K was made from k_b^{298}, by assuming an Eyring-type temperature dependence (Eq. 6). The extrapolated exchange rates (k_b^{265}) are compared in Table 3 with the averaged exchange rates of hydroxyl protons in compounds **3**, **4** and **5** published by Sandström et al.[7] Our extrapolated exchange rates appear to be up to four times higher than those measured by Sandström et al.[7] at 265 K. However, considering that Sandström and co-workers used a mixed solvent (85% H_2O–15% $(CD_3)_2CO$), purified the sugars on a ion-exchange resin prior to experiments and probably used a slightly less acidic pH (7.0 ± 0.5), such a difference is not unexpected.

From the k_b^{298} values reported in Table 3 it is also evident that exchange in trehalose is considerably faster than in sucrose. Moreover, the rate decreases with increasing concentration for sucrose but increases for trehalose. The exchange rates at low temperature were calculated from k_b^{298}, by applying an Eyring-type temper-

ature dependence, as previously done for methyl glucoside. Extrapolated values are compared in Table 3 with exchange rates that were measured with a saturation transfer method.[40,59] Our extrapolated k_b^{273} values are up to 15 times higher than those in literature, possibly owing to the difference in samples preparation and solvent composition in Ref. 40.

The dispersion curves of three maltose samples at the concentrations 5%, 10% and 20% w/w are shown in Figure 5. In each panel the highest curve corresponds to the relaxation rate at the longest pulse spacing. The shift towards low temperature of the $1/T_2$ maximum with increasing concentration is evident in Figure 5. This is due to an increase of the exchange rate. Note that the scale is different in each panel, since the maximum $1/T_2$ is proportional to $P_b\delta\omega$. The corresponding k_b^{298} values shown in Table 3 are quite high for all these samples, probably again owing to the contribution of the anomeric hydroxyl proton. This proton is the most acidic in these sugars because of the withdrawing effect of the ring oxygen and it is expected to exchange faster than ring protons.[13,51] Hills et al.[16] reported an exchange rate of $1800\ s^{-1}$ for a 2% maltoheptaose solution. The effect of concentration on exchange rate shown by maltose is likely to be present in maltoheptaose solution as well. Therefore, the much higher value of about $3000 \pm 60\ s^{-1}$ found here for the 19.8% sample is reasonably expected for a 10-fold increase of concentration.

3.4. Relaxation time

Unlike the other extracted parameters, T_{2b}^{298} is more difficult to interpret in polydisperse systems and a study of simulated polydisperse systems[20] has indicated that the extracted apparent value of T_{2b}^{298} depends in a complicated way on the efficiency of the fitting routine in different T_{2b}^{298} regimes, with the result that the apparent value is weighted towards the millisecond range where $1/T_{2b}^{298}$ is of the order of $\delta\omega_b^{298}$. Since in the systems studied here, the mobility of the carbohydrate OH protons is not expected to vary greatly within a given sample, the extracted values of T_{2b}^{298} should closely represent the sample average values weighted by amount.

In general, T_2 depends on the strength of the proton–proton dipolar interaction (both intra- and inter-molecular) and its time dependence. The strength of dipolar interaction is expected to be similar for all of the samples in this study, but the rate at which it fluctuates will depend on internal motions of the particular molecule and on its tumbling motion. A particular motion will be more effective in driving spin–spin relaxation the slower it is, therefore molecular tumbling and backbone motions of molecular chains are expected to be the dominant relaxation mechanisms, rather than the faster reorientation of the O–H bond around the C–O axis.

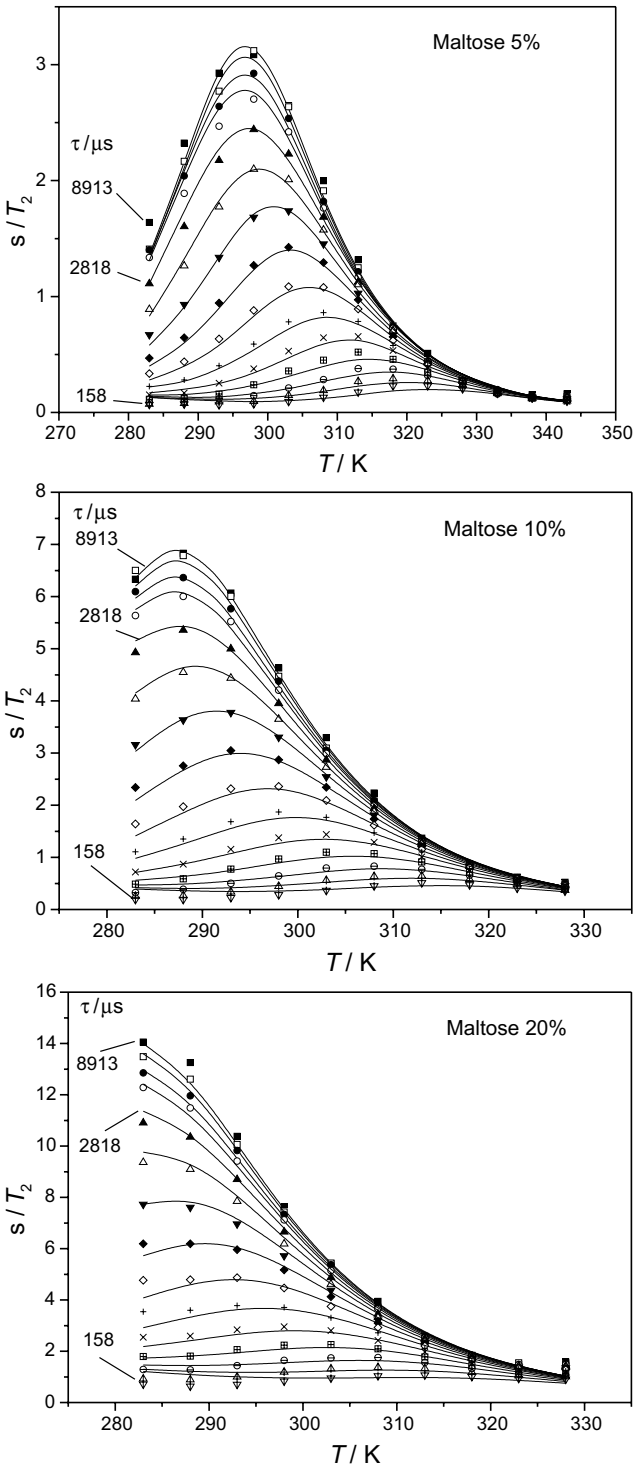

Figure 5. Relaxation rates of 5%, 10% and 20% w/w maltose solutions plotted as a function of temperature. Experimental data (symbols) and corresponding CR fits calculated using parameters from Tables 1–4 (solid lines).

The rate of tumbling depends on the effective size and the shape of the hydrated molecule. On the other hand, backbone motions depend on whether the molecule is a flexible chain or a more rigid ring. Consequently, T_{2b}^{298} is,

with $\delta\omega_b^{298}$, the parameter most closely related to conformation. This interpretation is supported by the observation that glucitol (**1**) and mannitol (**2**) have similar relaxation times, although high-resolution NMR[60] and molecular-dynamics simulations of glucitol (**1**) and mannitol (**2**) in aqueous solution show that the latter has a higher internal mobility for rotation around bonds than the former.

The T_{2b}^{298} values for methyl glycosides in Table 4 are all between 100 and 190 ms, while the values for the polyol samples were $\geqq$190 ms. This difference suggests that the mobility of the cyclic methyl glycosides is lower than that of the linear polyols. Although the concentration dependence has not been studied extensively for these samples, all available data suggest that concentration does play a role in determining the mobility of the sugar hydroxyl bond, since more concentrated samples have shorter T_{2b}, probably because molecular tumbling is slower. This is consistent with the results obtained for the polyols.

Given the high exchange rate of both trehalose samples and of 10% sucrose, an accurate determination of their spin–spin relaxation times was not possible, since relaxation is dominated by the exchange even at the lowest temperatures. T_{2b} of those samples was arbitrarily fixed prior to fitting, whereas for the 20% sucrose samples, the values of T_{2b}^{298} were set as free parameters (see Table 4) and found to be similar to those in methyl glycosides.

The relaxation time of 20% maltose (**12**) (~70 ms) is significantly shorter than for Me α-glucoside (**3**) (~117 ms). A decrease in T_{2b} with increasing concentration, corresponding to a decrease in mobility, was found also in this class of compounds. The value ~40 ms that gave the best fit for 19.8% maltoheptaose is the shortest found in this study. This would be consistent with slower tumbling of this large molecule and with slower conformational fluctuations of the longer chain.

The temperature dependence of T_{2b}^{298} was similar for all samples, and it was modelled by an Arrhenius activation energy, E_b in the range 10–30 kJ mol^{-1}.

4. Mechanism of proton exchange: a discussion

4.1. Cyclic concerted mechanism

The pH dependence of the exchange rate measured in methanol[20,61] and in carbohydrate[2,58] aqueous solutions is characteristic in being U-shaped, rather than V-shaped. The rapid increase of k at both low and high pH values, typical of acid–base catalysis, starts at both sides of a minimum, which is a plateau extended over few pH units at about neutral pH. The standard model for acid–base catalysis leads to Eq. (2)

$$\mathrm{ROH} + \mathrm{H_3O^+} \rightleftharpoons \mathrm{ROH_2^+} + \mathrm{H_2O}, \tag{2a}$$

$$\mathrm{ROH} + \mathrm{OH^-} \rightleftharpoons \mathrm{RO^-} + \mathrm{H_2O}, \tag{2b}$$

$$k_b = k_1[\mathrm{H_3O^+}] + k_2K_w/[\mathrm{H_3O^+}], \tag{2c}$$

where k_1 and k_2 are the rate constants corresponding to Eqs. 2a and 2b, respectively, K_w is the dissociation constant of water and k_b represents a pseudo-first-order rate constant. In order to account for the exchange rate versus pH curves in aqueous solution of proteins and nucleotides at pH close to neutral, a pH-independent water-catalysed term is often included.[62–64] Similarly, for neutral solutions of carbohydrates, the presence of an additional elementary step has been proposed[2,51,53,58,61] that would contribute to k_b with a pH-independent term k_3, so that Eq. 2c becomes Eq. 3.[61]

$$k_b = k_1[\mathrm{H_3O^+}] + k_2K_w/[\mathrm{H_3O^+}] + k_3[\mathrm{H_2O}]. \tag{3}$$

Hills[61] and Williams et al.[20] could account quantitatively for the observed plateau of exchange rate versus pH in methanol–water solutions at pH between 5 and 7 by considering the contribution from a neutral exchange mechanism. In the studies on protein solutions it has been pointed out[62] that the pH-independent term can arise from two different mechanisms: either (i) the water molecule behaves as a base to remove a labile proton directly, or (ii) there is a multiple-step equilibrium, including first a protonation, followed then by a deprotonation by OH^-, so that the rate, proportional to $[H^+]\times[OH^-]$, appears to be pH-independent. Harvey et al.[2] and Hills[61] suggested that for carbohydrate solutions the mechanism of exchange does not involve charge separation. This would imply that exchange happens via the mechanism (i) mentioned above. Although these authors do not justify their assumption, this is likely to be the preferred one in carbohydrates, where, given the high number of hydroxyl groups, extensive hydrogen bonding with water occurs at all times.

Harvey et al.[2] suggested that cyclic structures as in Figure 6 can form by chance in aqueous solutions and that subsequent concerted proton jumps can lead to pro-

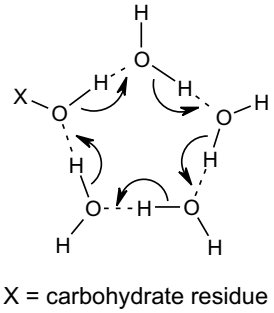

Figure 6. Cyclic concerted mechanism proposed for proton exchange at neutral pH, adapted from Ref. 2.

ton switching between solute and water. Chains of hydrogen bonds are known to form in carbohydrate crystals[65] and their crystal hydrates[66] and are expected to occur in solution too, although with a more dynamic character. From consideration of the sterical constraints and energetics of nonlinear H bonds, various authors[2,61] concluded that the cyclic structure should involve at least 5 molecules, as in Figure 6. From the concentration dependence of the exchange rate at pH close to neutral, Hills tried to discriminate among the many possible cyclic structures, both in methanol[61] and glucose solutions,[58] by correlating the exchange rate with the probability of random jumps of protons between oxygen nuclei for the different structures. He assumed that the exchange rate would be proportional to the probability of formation of such cyclic structures. However, it could be argued that the rate-determining step is not the formation of the H bond chain, but rather the transfer of a proton from the carbohydrate hydroxyl oxygen to a water oxygen. This corresponds to the formation of the H_3O^+ species, a defect that easily moves along the chain by flips of H bonds, thus exchanging the hydroxyl proton.

4.2. Exchange rates

Exchange rates for all sugar solutions examined here are within the range expected for carbohydrates.[13,16,20,67] Owing to the large change of k_b over the temperature range under investigation, and also owing to the sensitivity of this parameter to pH and adventitious catalysis, it is clear that a relatively large uncertainty should be attached to the absolute values reported in this study, referred to 298 K. It is important to underline that the uncertainty is not due to a poor fitting or failure of the CR model, but rather to the sometimes less than satisfactory reproducibility between runs. In fact, k_b was always determined in the CR fits with a quite narrow 95% confidence interval (usually well below 5%). It should also be recalled that the exchange rate k_b^{298} obtained from the fitting is the pre-exponential factor of the Eyring equation and contains contributions from both the enthalpic and entropic Eyring parameter. For this reason, when the experimental results have been presented in the previous sections, the search for trends of k_b^{298} was not over-emphasised, as it is in fact more informative to look directly at the Eyring parameters. This will be done in the next section.

4.3. Thermodynamics of exchange

The temperature-dependent study of the relaxation rate made it possible to obtain from the fitting, in addition to the exchange rate and its activation energy, E_a, two other parameters, that can be derived from k_b^{298} and E_a by applying the Eyring equation, namely the enthalpy and entropy of activation for the exchange process. The enthalpy of activation, $\Delta^{\ddagger}H^{\ominus}$, represents the energy difference between reacting species and the activated complex and it depends not only on the energy required for bond-breaking and bond-formation, but also on the extent of solvation in the two states.[68] The entropy of activation, $\Delta^{\ddagger}S^{\ominus}$, depends on the steric requirements during the encounter of the reactants and the stricter they are, the more negative is $\Delta^{\ddagger}S^{\ominus}$.[69] The loss or gain of degrees of freedom of the solvent is also included in this term.[68] The enthalpies and entropies of activation obtained for each class of small sugars are reported in Table 3, together with the k_b^{298} values. Enthalpies of activation, $\Delta^{\ddagger}H^{\ominus}$, in the range 50–70 kJ mol^{-1}, are extracted with similar uncertainties in all samples and decrease with increasing concentration. The fact that $\Delta^{\ddagger}H^{\ominus}$ values are much higher than the order of enthalpy of formation of a hydrogen bond (~20 kJ mol^{-1}), gives further support to the idea that the rate-determining step of the exchange process is not the formation of the cyclic water structures around the hydroxyl protons, but rather a bond-dissociation step. In some hydrogen isotope exchange studies in protein solutions[63,70] activation energies were measured for the acid, base and water catalysis and gave values of about 60, 70 and above 80 kJ mol^{-1}, respectively. The exchange in carbohydrate solution is expected to have similar values of activation energy. The entropies of activation reported in Table 3 vary between −10 and 60 J K^{-1} mol^{-1}. At 20% concentration, polyols and maltose oligosaccharides have the lowest $\Delta^{\ddagger}S^{\ominus}$ values that become negative in some samples. It can be anticipated here that $\Delta^{\ddagger}S^{\ominus}$ values in maltodextrins are found to be even more negative (manuscript in preparation) so that a trend of progressive conformational constraints from the chain length and concentration can be adduced to explain the difference between the oligomers and the mono- or disaccharides. The results for the polyols would mean that the steric changes required during formation of the activation complex are much more demanding for these molecules than for cyclic sugars. A larger entropy loss is required for going to the activation state from a mobile acyclic chain than from a cyclic conformation.

Glucitol and maltose were the only two sugars studied in a slightly wider concentration range 5–20% w/w. It was found (Table 3) that the exchange rates for the two compounds had an opposite dependence on concentration, as k_b^{298} was decreasing with increasing concentration for glucitol, while it was increasing for maltose. However, if the actual Eyring parameters are considered instead of k_b^{298}, it is evident that in fact both sugars have decreasing $\Delta^{\ddagger}H^{\ominus}$ and $\Delta^{\ddagger}S^{\ominus}$ values with increasing concentration.

The large difference in exchange rate shown by glucitol and mannitol (Table 3) was surprising too. Molecular-dynamics simulations and NMR studies of chemical shifts and coupling constants[60] demonstrated that

internal rotation around bonds is higher in glucitol than mannitol, and also that water has a longer residence time in the proximity of mannitol. It is however difficult to judge how these characteristics would favour the exchange process, especially bearing in mind that the time scales of NMR events and MD simulations are many order of magnitude apart. Interestingly, from the analysis of the Eyring parameters it can be seen that although mannitol has a higher enthalpy of activation, the entropy of activation is larger and more positive, and it does not become negative even at the highest concentration. This suggests that the steric entropic factors, rather than the energy barriers, are critical for the exchange in these samples.

The stereospecificity of hydration and importance of solvent structuring around carbohydrate molecules have been studied with a variety of techniques.[23,25,30,31,33–35,37–39,71,72] The compatibility of a sugar with hydration requirements and its interaction with the solvent certainly have implications for a series of solution properties, like solvation, solubility, viscosity, reactivity and for chemical exchange too. It would therefore be of considerable interest to understand what is the effect of hydroxyl conformation of the sugar rings on the exchange process. In the case of the methyl glycosides, our results gave a clear indication that some variations among samples are conformation dependent, especially if the data about the number of available exchangeable protons, P_b, are considered together with the actual exchange rates (Tables 2 and 3). Harvey et al.[51] suggested that, compared with small polyols, effective exchange in cyclic aldoses might be impeded by the formation of smaller hydrogen-bond cyclic chains involving adjacent hydroxyl groups. Our results are at variance with this assertion since we found that glycerol and glycol exchange faster than acyclic hexitols, but slower than cyclic sugars in solutions having comparable P_b. Although our measurements show differences in the exchange rates, it proved impossible to make a direct correlation with the stereochemistry. The observed dispersion represents an averaged relaxation rate and the molecular parameters are, similarly, averaged. While for some systems this does not represent an obstacle, for samples where the conformational differences are small this approach is less informative than other techniques, for example, high-resolution NMR or MD, could be.

4.4. Conclusions

The CR exchange model is suitable to interpret the ^1H T_2-dispersion curves for water protons in solutions of small sugars. The model accounts well for the enhancement of the observed water relaxation rate in terms of molecular parameters related to the identity, concentration and mobility of the labile groups, as well as to the exchange rate itself and the CPMG pulse spacing. This implies that it is unnecessary to include a 'bound' water pool in the model. The statistical evaluation of fitting output, routinely run, reveals that the nonlinear regression method for data fitting is successful and that the global fitting approach (that is, simultaneous fit of dispersion curves at all temperatures) is advantageous and therefore preferable to separate fits of individual dispersion curves.

The CR parameters related to the carbohydrate solute OH protons have been characterised and are found to be in agreement with literature data. Chemical-shift differences, $\delta\omega_b^{298}$, are about 1 ppm, the intrinsic relaxation time, T_{2b}, of the order of hundreds of milliseconds, and the exchange rate, (k_b), in the kHz region. CR parameters values are generally quite similar among the sugars studied here, nevertheless effects of cyclic conformation, hydroxyl conformation and chain length could be detected by changes among sugars classes. Sometimes these effects, however, were too small to be interpreted with confidence and improvements in the instrumental set-up to reduce the S/N ratio would be necessary if a more accurate determination of the relaxation parameters were to be obtained.

5. Experimental

5.1. Sample preparation for NMR studies

Commercial samples of analytical grade were used without further purification. The solutions were prepared by weight for both sugar and distilled deionised water (resistance greater than 18 MW; Elgastat UHQ II deioniser). Crystallisation water, when present, was taken into consideration in calculating the total water amount. The solutions were stirred until the sugar was completely dissolved. Concentrations are expressed in weight % of solute in the total solution (% w/w). The pH was measured for all samples and found to be between 6.0 and 7.0. Note that all sugars in this study are the D-enantiometers, therefore the D is generally omitted throughout this article.

The short name, chemical name, and supplier of the compounds studied are as follows: β-maltose, 4-*O*-α-D-glucopyranosyl-D-glucopyranoside, (monohydrate) Sigma; maltotriose, α-D-glucopyranosyl-(1→4)-α-D-glucopyranosyl-(1→4)-D-glucose, Sigma; maltoheptaose, α^5-D-glucopyranosyl-(1→4)-[α-D-glucopyranosyl-(1→4)]5-D-glucopyranoside, (Lyophilisat) Boehringer Mannheim; α,α-trehalose, α-D-glucopyranosyl α-D-glucopyranoside, (dihydrate) Sigma; sucrose, β-D-fructofuranosyl α-D-glucopyranoside Sigma; methyl α-D-xylopyranoside, Sigma; methyl β-D-xylopyranoside, Sigma; methyl α-D-glucopyranoside, Lancaster; methyl β-D-glucopyranoside, (hemihydrate) Lancaster; methyl α-D-galactopyranoside, Sigma; methyl β-D-galactopyranoside, Sigma; methyl β-D-arabinopyranoside, Sigma;

(ethylene) glycol, 1,2-ethanediol, Fisons; glycerol,1,2,3-propanetriol, Fisher; glucitol, D-glucitol, Lancaster; mannitol, D-mannitol, Lancaster.

5.2. NMR spectroscopy

5.2.1. Spectrometer system. All measurements were carried out on a Bruker WP80 SY electromagnet (1.88 T) operating at about 80 MHz for ^{1}H resonance, which was stabilised with a flux stabiliser and shimmed. The spectrometer (Resonance Instruments, Wilton, Oxfordshire, UK) was interfaced to a PC allowing experiments to be automated via a user-specified macro that can control the temperature profile, the pulse spacing (τ), the spectrometer frequency, data collection and initial data processing. Typical 90° pulse lengths were 10–15 μs. A Bruker WP80 probe was modified in order to incorporate a computer-controlled Peltier heating–cooling device.[73] This was located inside the probe body and attached to a copper can filled with perfluoromethyldecalin (as a heat-transfer agent) into which the sample tube was introduced. In order to improve heat transfer the perfluoromethyldecalin was stirred by gas bubbling, which was computer-controlled and shut off during acquisition of the NMR signal. The NMR tubes were 5-mm, thin walled, glass tubes (Aldrich, 507-PP-7). The sample volume was ca. 0.1 mL and the tube positioned so that the whole sample was located within the probe coil. This arrangement gave a well-behaved NMR signal and also facilitated rapid response of the sample to temperature changes, owing to its small volume. The temperature could be controlled to within ±0.2 K within the range 278–343 K.

5.2.2. NMR data acquisition. The ^{1}H spin–spin relaxation times (T_2) were measured with the CPMG sequence $90°_x$–τ–$[180°_y$–τ–echo–$\tau]_n$ as a function of temperature and pulse spacing τ. Generation of the pulse sequence, setting up of parameters, experiment procedures and data collection were completely automated by user-specified macros written in Turbo Pascal (Borland PASCAL for Windows) and implemented within the Resonance Instrument[74] operating system. In T_2-dispersion experiments, the pulse spacing τ of the CPMG sequence was varied between 158 and 8913 μs over 15 values, equally spaced on a logarithmic scale. The number of echoes, n was chosen for each τ to ensure that a stable baseline was reached after the signal had decayed. n varied from 31,646 for the shortest τ = 158 μs up to 560 μs for the longest τ = 8.9 ms so that the total duration of a scan was always 10 s. Only the top point of each echo maximum was recorded, Two scans were recorded for each τ by applying a 30 s recycle delay between sequences to avoid saturation, and using phase cycling to improve the signal-to-noise ratio. CPMG echo envelopes were fitted to an exponential function with a nonlinear regression method based on the Levenberg–Marquardt algorithm.[74] In addition to T_2, a statistical estimate of the goodness of fit, $\chi_v = s^2/\sigma^2$ was computed, where s^2 is the variance of the fit and σ^2 is the variance of the noise measured from the last 100 points of the out-of-phase signal. The relative error in T_2 was < 2%. The decays were always found to be single exponential, indicating that the self-diffusion of water and the exchange of protons between bulk water and solute were sufficiently rapid for the water response to be characterised by a single averaged relaxation time. The CPMG sequence was nested in programmed τ and T loops in order to record automatically complete dispersions at different temperatures.

The relaxation experiments carried out were measurements of dispersion curves, that is, relaxation rate ($1/T_2$) versus pulse spacing (τ) as a function of temperature (T). The dispersion curves were measured at a series of temperatures from 283 K up to 343 K, in steps of 5 K. Fifteen minutes were allowed for stabilisation of the sample at each temperature. A similar set of dispersion curves was measured for the relaxation times, T_{2a} of the water used to prepare the solutions.

5.3. Fitting the dispersion curves

In a typical experiment, the set of dispersion curves ($1/T_2(\tau, T)$) consists of 195 points (15τ values, each at 13 different temperatures). The set of dispersions was fitted as function of both pulse spacing and temperature simultaneously, using Eq. 1. The fit was carried out with a user-defined macro (SPSS 10 for Windows, SPSS Inc.) that incorporated the Levenberg–Marquardt algorithm for the nonlinear regression method.[75] The formulation given by Davis et al.[76] was used to code the function f_{CR}. P_b was assumed to be independent of temperature. The temperature dependence of T_{2b} was given by an Arrhenius-type equation, which can be written in the form

$$T_{2b}(T) = T_{2b}^{298} \exp\left[\frac{E_b}{R}\left(\frac{1}{T} - \frac{1}{298\ \mathrm{K}}\right)\right], \qquad (4)$$

where T_{2b}^{298} is the relaxation time at 298 K and E_b the activation energy. In general, on carrying out the fitting procedure it was found that the iterations converged more rapidly and the program was more stable if the temperature-independent parameters were defined for 298 K (i.e., near the middle of the experimental temperature window) rather than for infinite temperature.

The temperature dependence of k_b was expressed by an Eyring-type equation

$$k_b(T) = \frac{k_B T}{h} \exp[\Delta^{\ddagger} S^{\ominus}/R] \exp[-\Delta^{\ddagger} H^{\ominus}/RT], \qquad (5)$$

where $\Delta^{\ddagger}S^{\ominus}$ and $\Delta^{\ddagger}H^{\ominus}$ are the entropy and enthalpy of activation, respectively. For the purposes of fitting, the parameter k_b^{298}, the exchange rate at 298 K, was introduced by writing Eq. 5 in the form Eq. 6

$$k_b(T) = k_b^{298}\frac{T}{298\ \mathrm{K}}\exp\left[\frac{-\Delta^{\ddagger}H^{\ominus}}{R}\left(\frac{1}{T}-\frac{1}{298\ \mathrm{K}}\right)\right]. \quad (6)$$

A linear temperature dependence was assumed for the chemical-shift difference,

$$\delta\omega_b(T) = \delta\omega_b^{298} + \Delta\delta\omega_b(T - 298\ \mathrm{K}). \quad (7)$$

The outputs of the fit are the parameters: P_b, T_b^{298}, E_b, k_b^{298}, $\Delta^{\ddagger}H^{\ominus}$, $\delta\omega_b^{298}$, $\Delta\delta\omega_b$ together with error statistics, including 95% confidence limits of the parameters.

Acknowledgements

This work has been carried out with financial support from the Commission of the European Communities, Agriculture and Fisheries (FAIR) specific RTD programme, CT 96 1015, 'Mixed Biopolymers Mechanism and Application of Phase Separation'. It does not necessarily reflect its views and in no way anticipates the Commission's future policy in the area. The authors would like to thank Roy Noakes and Barry Firth for technical support. D.F. would like to thank the University of Trieste for a grant and Unilever R&D Colworth for financial support.

References

1. Duus, J. O.; Gotfredsen, C. H.; Bock, K. *Chem. Rev.* **2000**, *100*, 4589–4614.
2. Harvey, J. M.; Symons, M. C. R. *J. Solution Chem.* **1978**, *7*, 571–586.
3. Poppe, L.; van Halbeek, H. *J. Am. Chem. Soc.* **1991**, *113*, 363–365.
4. Poppe, L.; van Halbeek, H. *J. Am. Chem. Soc.* **1992**, *114*, 1092–1094.
5. Pearce, C. M.; Sanders, J. K. M. *J. Chem. Soc., Perkin Trans. 1* **1994**, 1119–1124.
6. Adams, B.; Lerner, L. E. *Magn. Reson. Chem.* **1994**, *32*, 225–230.
7. Sandstrőm, C.; Baumann, H.; Kenne, L. *J. Chem. Soc., Perkin Trans. 2* **1998**, 809–815.
8. Sandstrőm, C.; Baumann, H.; Kenne, L. *J. Chem. Soc., Perkin Trans. 2* **1998**, 2385–2393.
9. Sandstrőm, C.; Magnusson, G.; Nilsson, U.; Kenne, L. *Carbohyd. Res.* **1999**, *322*, 46–56.
10. Ivarsson, I.; Sandstrőm, C.; Kenne, L. *J. Chem. Soc., Perkin Trans. 2* **2000**, 2147–2152.
11. Bekiroglu, S.; Sandstrőm, C.; Norberg, T.; Kenne, L. *Carbohydr. Res.* **2000**, *328*, 409–418.
12. Gordalla, B. C.; Zeidler, M. D. *Mol. Phys.* **1991**, *74*, 975–984.
13. Hills, B. P.; Wright, K. M.; Belton, P. S. *Mol. Phys.* **1989**, *67*, 1309–1326.
14. Hills, B. P.; Takacs, S. F.; Belton, P. S. *Mol. Phys.* **1989**, *67*, 903–918.
15. Hills, B. P.; Takacs, S. F.; Belton, P. S. *Mol. Phys.* **1989**, *67*, 919–937.
16. Hills, B. P.; Cano, C.; Belton, P. S. *Macromolecules* **1991**, *24*, 2944–2950.
17. Venu, K.; Denisov, V. P.; Halle, B. *J. Am. Chem. Soc.* **1997**, *119*, 3122–3134.
18. Liepinsh, E.; Otting, G. *Magn. Reson. Med.* **1996**, *35*, 30–42.
19. Carver, J. P.; Richards, R. E. *J. Magn. Reson.* **1972**, *6*, 89–105.
20. Williams, M. A. K.; Keenan, R. D.; Halstead, T. K. *Magn. Reson. Chem.* **1998**, *36*, 163–173.
21. Pigman, W. *The Carbohydrates—Chemistry Biochemistry Physiology*; Academic: New York, 1957.
22. Collins, P. M.; Ferrier, R. J. *Monosaccharides—Their Chemistry and Their Roles in Natural Products*; John Wiley & Sons: Chichester, 1995.
23. Tait, M. J.; Sugget, A.; Franks, F.; Ablett, S.; Quickenden, P. A. *J. Solution Chem.* **1972**, *1*, 131–151.
24. Kabayama, M. A.; Patterson, D.; Piche, L. *Can. J. Chem.* **1958**, *36*, 557–562.
25. Kabayama, M. A.; Patterson, D. *Can. J. Chem.* **1958**, *36*, 563–573.
26. Hollenberg, J. L.; Hall, D. O. *J. Phys. Chem.* **1983**, *87*, 695–696.
27. Franks, F. *Pure Appl. Chem.* **1987**, *59*, 1189–1202.
28. Franks, F.; Lillford, P. J.; Robinson, G. *J. Chem. Soc., Faraday Trans. 1* **1989**, *85*, 2417–2426.
29. Brady, J. W. *J. Am. Chem. Soc.* **1989**, *111*, 5155–5165.
30. Galema, S. A.; Blandamer, M. J.; Engberts, J. B. F. N. *J. Am. Chem. Soc.* **1990**, *112*, 9665–9666.
31. Galema, S. A.; Hoiland, H. *J. Phys. Chem.* **1991**, *95*, 5321–5326.
32. Ha, S. H.; Gao, J. L.; Tidor, B.; Brady, J. W.; Karplus, M. *J. Am. Chem. Soc.* **1991**, *113*, 1553–1557.
33. Hajduk, P. J.; Horita, D. A.; Lerner, L. E. *J. Am. Chem. Soc.* **1993**, *115*, 9196–9201.
34. Galema, S. A.; Engberts, J. B. F. N.; Hoiland, H.; Forland, G. M. *J. Phys. Chem.* **1993**, *97*, 6885–6889.
35. Galema, S. A.; Howard, E.; Engberts, J. B. F. N.; Grigera, J. R. *Carbohydr. Res.* **1994**, *265*, 215–225.
36. Cheetham, N. W. H.; Lam, K. *Carbohydr. Res.* **1996**, *282*, 13–23.
37. Liu, Q.; Brady, J. W. *J. Am. Chem. Soc.* **1996**, *118*, 12276–12286.
38. Liu, Q.; Brady, J. W. *J. Phys. Chem. B* **1997**, *101*, 1317–1321.
39. Stenger, J.; Cowman, M.; Eggers, F.; Eyring, E. M.; Kaatze, U.; Petrucci, S. *J. Phys. Chem. B* **2000**, *104*, 4782–4790.
40. Adams, B.; Lerner, L. *J. Am. Chem. Soc.* **1992**, *114*, 4827–4829.
41. Mathlouthi, M.; Luu, D. V. *Carbohydr. Res.* **1980**, *81*, 203–212.
42. Duda, C. A.; Stevens, E. S. *J. Am. Chem. Soc.* **1990**, *112*, 7406–7407.
43. Engelsen, S. B.; Dupenhoat, C. H.; Perez, S. *J. Phys. Chem.* **1995**, *99*, 13334–13351.
44. Immel, S.; Lichtenthaler, F. W. *Liebigs Ann. Chem.* **1995**, 1925–1937.
45. Engelsen, S. B.; Perez, S. *J. Mol. Graphics Modell.* **1997**, *15*, 122–131.
46. Liu, Q.; Schmidt, R. K.; Teo, B.; Karplus, P. A.; Brady, J. W. *J. Am. Chem. Soc.* **1997**, *119*, 7851–7862.

47. Magazu, S.; Migliardo, P.; Musolino, A. M.; Sciortino, M. T. *J. Phys. Chem. B* **1997**, *101*, 2348–2351.
48. Batta, G.; Kover, K. E. *Carbohydr. Res.* **1999**, *320*, 267–272.
49. Engelsen, S. B.; Perez, S. *J. Phys. Chem. B* **2000**, *104*, 9301–9311.
50. Magazu, S.; Villari, V.; Migliardo, P.; Maisano, G.; Telling, M. T. F. *J. Phys. Chem. B* **2001**, *105*, 1851–1855.
51. Harvey, J. M.; Symons, M. C. R.; Naftalin, R. J. *Nature* **1976**, *261*, 435–436.
52. Bociek, S.; Franks, F. *J. Chem. Soc., Faraday Trans. 1* **1979**, *75*, 262–270.
53. Symons, M. C. R.; Benbow, J. A.; Harvey, J. M. *Carbohydr. Res.* **1980**, *83*, 9–20.
54. Harvey, J. M.; Jackson, S. E.; Symons, M. C. R. *Chem. Phys. Lett.* **1997**, *47*, 440–441.
55. Busfield, W. K.; Ennis, M. P.; McEwen, I. J. *Spectrochim. Acta* **1973**, *29A*, 1259–1264.
56. Chidichimo, G.; Imbardelli, D.; Longeri, M.; Saupe, A. *Mol. Phys.* **1988**, *65*, 1143–1151.
57. Nagy, P. I.; Dunn, W. J.; Alagona, G.; Ghio, C. *J. Am. Chem. Soc.* **1992**, *114*, 4752–4758.
58. Hills, B. P. *Mol. Phys.* **1991**, *72*, 1099–1121.
59. Adams, B.; Lerner, L. *J. Magn. Reson.* **1992**, *96*, 604–607.
60. Franks, F.; Dadok, J.; Ying, S.; Kay, R. L.; Grigera, J. R. *J. Chem. Soc., Faraday Trans.* **1991**, *87*, 579–585.
61. Hills, B. P. *J. Chem. Soc., Faraday Trans.* **1990**, *86*, 481–487.
62. Jeng, M. F.; Englander, S. W. *J. Mol. Biol.* **1991**, *221*, 1045–1061.
63. Bai, Y. W.; Milne, J. S.; Mayne, L.; Englander, S. W. *Proteins—Struct. Funct. Genet.* **1993**, *17*, 75–86.
64. Bai, Y. W.; Englander, J. J.; Milne, J. S.; Mayne, L.; Englander, S. W. *Energetics Biol. Macromol.* **1995**, *259*, 344–356.
65. Jeffrey, G. A. *Adv. Enzymol. Relat. Areas Mol. Biol.* **1992**, *65*, 217–254.
66. Kitchin, S. J.; Halstead, T. K. *Solid State Nucl. Magn. Reson.* **1996**, *7*, 27–44.
67. Derbyshire, W.; Duff, I. D. *J. Chem. Soc., Faraday Discuss.* **1974**, *57*, 243–254.
68. Engberts, J. B. F. N.. In *Water: A Comprehensive Treatise*; Franks, F., Ed.; Plenum: New York, 1979, pp 139–237.
69. Atkins, P. W. *Physical Chemistry*, 5th ed.; OUP: Oxford, 1994; p 947.
70. Gregory, R. B.; Crabo, L.; Percy, A. J.; Rosenberg, A. *Biochemistry* **1983**, *22*, 910–917.
71. Cheetham, N. W. H.; Lam, K. *Aust. J. Chem.* **1996**, *49*, 365–369.
72. A., S. *J. Solution Chem.* **1976**, *5*, 33–46.
73. Williams, M. A. K.; Fabri, D.; Halstead, T. K.; Hubbard, C. D. *Instrum. Sci. Technol.* **2001**, *29*, 367–382.
74. Press, W.; Flannery, B.; Teukolsky, S.; Vetterling, W. *Numerical Recipes: the Art of Scientific Computing*; Cambridge University Press: Cambridge, 1986.
75. Marquardt, D. W. *J. Soc. Ind. Appl. Math.* **1963**, *11*, 431–441.
76. Davis, D. G.; Perlman, M. E.; London, R. E. *J. Magn. Reson. Ser. B* **1994**, *104*, 266–275.